PROCEEDINGS OF THE INTERNATIONAL CONFERENCE NANOMATERIALS: APPLICATIONS AND PROPERTIES
Vol. **1** No 1, 01NNBM02(3pp) (2012)

Sol-Gel Synthesis and Characterization of Cerium Substituted Calcium Hydroxyapatite

I. Bogdanoviciene[1,*], M. Misevicius[1], L. Bauermeistere[2], A. Viksna[2],
K.A. Gross[3], A. Beganskiene[1], A. Kareiva[1]

[1] *Department of General and Inorganic Chemistry, Vilnius University, LT-03225 Vilnius, Lithuania*
[2] *Faculty of Chemistry, University of Latvia, LV-1013 Riga, Latvia*
[3] *Institute of Biomaterials and Biomechanics, Riga Technical University, LV-1048 Riga, Latvia*

(Received 15 February 2012; published online20 June 2012)

In this study, an aqueous sol-gel chemistry route based on phosphoric acid as the phosphorus precursor, calcium acetate monohydrate and cerium (III) nitrate hexahydrate as source of calcium and cerium ions, respectively, have been used to prepare cerium-substituted calcium hydroxyapatite (CHAp) powders. The tartaric acid was used as complexing agent in the sol-gel processing. The final products were obtained by calcination of the dry precursor gels for 5 h at 1000 °C. The phase transformations, composition, and structural changes in the polycrystalline samples were studied by infrared spectroscopy (IR), X-ray powder diffraction analysis (XRD), scanning electron microscopy (SEM), UV-visible reflection spectroscopy and luminescence measurements. It was demonstrated, however, that the high substitution of calcium by cerium does not proceed in the CHAp. The reflectance spectra of Ce substituted CHAp show nearly 100% reflection in the wavelength range of 450-800 nm. The luminescent properties of these samples were also investigated.

Keywords: Calcium hydroxyapatite, Sol-gel processing, Cerium substitution effects.

PACS numbers: 61.05.cp, 78.30.Hv

1. INTRODUCTION

Calcium hydroxyapatite, $Ca_{10}(PO_4)_6(OH)_2$, commonly referred to as CHAp, is one of the calcium phosphate based bioceramic material which makes up the majority of the inorganic components of human bones and teeth. Synthetic CHAp is known to be one of most important implantable materials due to its biocompatibility, bioactivity and osteoconductivity coming from the analogy to the mineral components of natural bones. For the use in medical practice, the CHAp ceramics have been conventionally strengthened and toughened in the form of granules and dense or porous ceramics composites, coatings, whiskers, nanorods and different pieces with complex shapes. Although these materials can closely replicate the structure of human bone, the improvement of properties of the materials is still very much desirable [1].

The specific chemical structural and morphological properties of CHAp bioceramics are highly sensitive to the changes in chemical composition and processing conditions [2-5]. However, the stability of crystal structure of CHAp is higher than that of natural apatite. CHAp is difficult to degrade in living body. Most natural apatite is non-stoichiometric because of the presence of minor constituents such as cations (Mg^{2+}, Mn^{2+}, Zn^{2+}, Na^+, Sr^{2+}) or anions (HPO_4^{2-} or CO_3^{2-}) [6, 7]. The traces of metal ions introduced in apatite structure can effect on the lattice parameters, the crystallinity, dissolution kinetics and other physical properties of apatite. The reports regarding the substitution of Ca^{2+} ions by bivalent or trivalent metal ions attracted attention during the past few years [8–10]. However, according to these reports some metal ions did not enter the crystal lattice of CHAp. It was also suggested that lanthanide elements might play an important role in enamel demineralization reduction [11].

Over the last few decades, the sol-gel technique has been used to prepare a variety of mixed-metal nanoporous oxides, nanomaterials, nanoscale architectures and organic-inorganic hybrids [12-15]. It has been demonstrated that sol-gel process offers considerable advantages such as better mixing of the starting materials and excellent chemical homogeneity in the final product. Moreover, the molecular level mixing and the tendency of partially hydrolyzed species to form extended networks facilitate the structure evolution thereby lowering the crystallization temperature. Recently, for the preparation of calcium hydroxyapatite samples with different properties an aqueous sol-gel processing route was elaborated [16-18]. The main aim of this study was to investigate cerium substitution effects in $Ca_{10-x}Ce_x(PO_4)_6(OH)_2$ synthesized using an environmentally friendly aqueous sol-gel method.

2. EXPERIMENTAL PART

Calcium hydroxyapatite powders substituted by cerium $Ca_{10-x}Ce_x(PO_4)_6(OH)_2$ having different concentrations of cerium (x = 0.01; 0.025; 0.05; 0.1; 0.5 and 1.0) were prepared by aqueous sol-gel method. In the sol-gel process $Ca(CH_3COO)_2{\cdot}H_2O$ (≥ 99 %, Fluka), phosphoric acid H_3PO_4 (85%, Eurochemical), tartaric acid $C_4H_6O_6$ (99,5 %, Aldrich), cerium (III) nitrate hexahydrate $Ce(NO_3)_3{\cdot}6H_2O$ (99,9 %, Merck) were used. Firstly, calcium acetate monohydrate and cerium (III) nitrate hexahydrate were dissolved in small amount of distilled water. Secondly, phosphoric and tartaric acids were added to the solution of metals. The resulting solution was vigorously stirred for 12 h at 65 ˚C tem-

* irma.bogdanoviciene@gmail.com

perature. Obtained sol was concentrated under evaporation till the transparent gel has formed. Further, the gel was dried for 24 h at 100 ˚C and then calcined for 5 h at 800 ˚C in air. The powders were grinded in agate mortar to increase the homogeneity and additionally calcined for 5 h at 1000 ˚C in air.

X-ray diffraction analysis (XRD) was performed on a Bruker AXE D8 Focus diffractometer with a LynxEye detector using Cu Kα radiation. Infrared spectra of samples in KBr pellets were recorded with a Bruker Equinox 55/S/NIR FTIR spectrometer (resolution 1 cm-1). The particle size and morphology of the resultant $Ca_{10-x}Ce_x(PO_4)_6(OH)_2$ powders were examined using FE-SEM Zeiss Ultra 55 scanning electron microscope with In-Lens detector. UV-Vis diffuse reflectance spectra were recorded on Perkin-Elmer Lambda 35 UV-Vis spectrophotometer with an integrated 50 mm sphere attachment. Investigation of luminescent properties was performed with PerkinElmer LS-55 fluorescence spectrometer.

3. RESULTS AND DISCUSSION

The XRD patterns of cerium substituted compounds $Ca_{10-x}Ce_x(PO_4)_6(OH)_2$ (x = 0.01; 0.025; 0.05; 0.1; 0.5 and 1.0) obtained at 1000 °C are shown in Fig. 1.

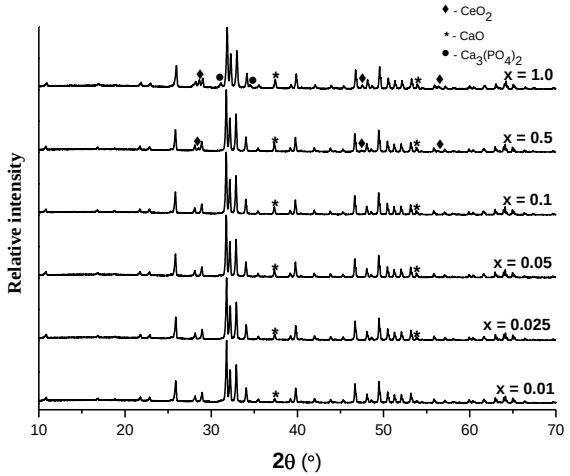

Fig. 1 – XRD patterns of $Ca_{10-x}Ce_x(PO_4)_6(OH)_2$ (x=0.01; 0.025; 0.05; 0.1; 0.5 and 1.0) powders synthesized by sol–gel method and annealed at 1000 ^{0}C for 5 h

As seen, the XRD patterns of CHAp with low concentrations of cerium (x = 0.01; 0.025; 0.05 and 0.1) revealed that the main crystalline component in the synthesis products is CHAp and only minor amount of calcium oxide could be detected. The obtained XRD patterns are in a good agreement with the reference data for $Ca_{10}(PO_4)_6(OH)_2$ (PDF [72-1243]) and CaO (PDF [37-1497]). With increasing concentration of cerium (x = 0.5 and 1.0), however, the formation of cerium oxide CeO2 (PDF [78-694]) and calcium phosphate Ca3(PO4)2 (PDF [86-1585]) phases occurs.

The IR spectra of the $Ca_{10-x}Ce_x(PO_4)_6(OH)_2$ samples are shown in Fig. 2. As was expected, all IR spectra are very similar. The absorbing bands indicate the formation of a typical HA structure containing sharp O–H and P–O peaks. The spectra of these samples clearly show the bands of a significant intensity at 1048 cm-1 and 1092 cm-1. These bands arise due to the factor group splitting of the v3 fundamental vibrational mode of the PO4 3- tetrahedral. The bands at ~962 cm-1 and at ~570–602 cm-1 correspond to symmetric stretching modes v1 and antisymmetric bending modes v4 P–O vibration of the phosphate groups respectively [19]. The peak observed at 630 cm-1, assigned in hydroxyapatite spectra to the O-H group vibrational mode and band of the stretch vibration mode of OH group in apatite structure at 3573 cm-1 is well visible, surface OH band at 3644 cm-1 also appears.

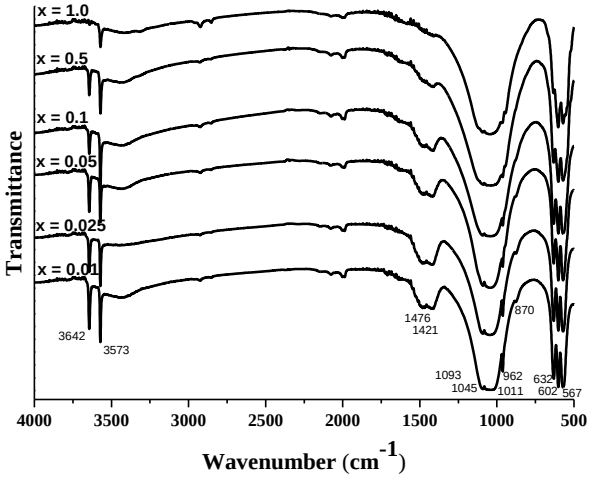

Fig. 2 – IR spectra of Ca10-xCex(PO4)6(OH)2 (x=0.01; 0.025; 0.05; 0.1; 0.5 and 1.0) powders synthesized by sol–gel method and annealed at 1000 0C for 5 h

The observed ν_3 carbonate bands at 1480 cm^{-1}, 1420 cm^{-1} and the ν_2 mode at 873 cm^{-1} suggest that part of PO_4^{3-} in CHAp is substituted by CO_3^{2-}. The carbonate might come from the atmosphere carbon dioxide which combined into the crystal structure during dissolving, stirring, reaction and the calcination processes [20].

Fig. 3 shows the representative SEM micrograph of cerium substituted CHAp sample.

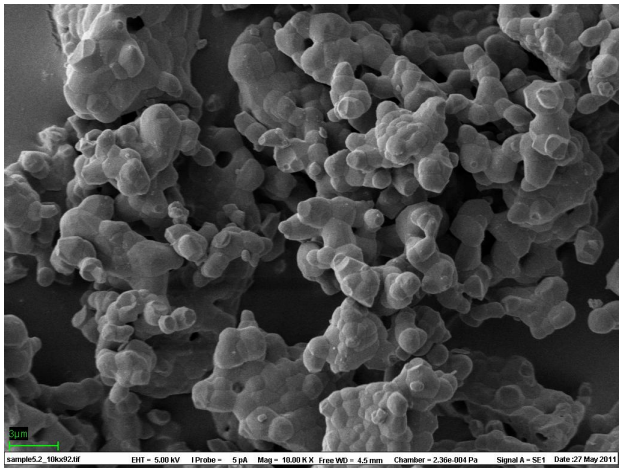

Fig. 3 – SEM micrograph of $Ca_{9.0}Ce_{1.0}(PO_4)_6(OH)_2$ powders synthesized at 1000 °C

SEM analysis data showed that cerium substituted CHAp samples are composed of the plate-like crystals with size of 0.5-1 μm. However, some of particles are close to nanometre dimensions. These nanograins show

tendency to form larger agglomerates. The SEM results also suggest that obtained cerium substituted CHAp crystallites are homogeneous with small particle size distribution.

The luminescent properties of these samples were also investigated. Fig. 4 shows the emission spectra of sol-gel derived cerium substituted CHAp samples.

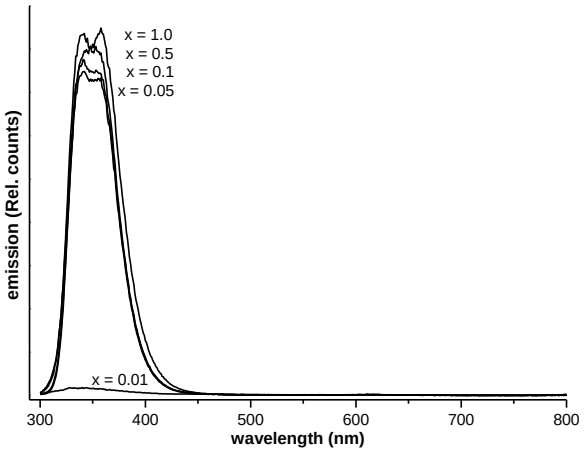

Fig. 4 – Emission spectra of $Ca_{10-x}Ce_x(PO_4)_6(OH)_2$ (x = 0.01; 0.05; 0.1; 0.5 and 1.0) powders synthesized by sol–gel method and annealed at 1000°C for 5 h

The position of the broad emission band at around 350 nm is almost independent on the Ce concentration, however, the intensity of photoluminescence peak slightly depends on the cerium concentration.

4. CONCLUSIONS

Cerium substituted calcium hydroxyapatite Ca10-xCex(PO4)6(OH)2 samples were synthesized using sol–gel method. The results of X-ray diffraction analysis showed the formation of almost single CHAp phase at low concentrations of cerium (x = 0.01; 0.025; 0.05 and 0.1). With further increasing amount of cerium (x = 0.5 and 1.0) the formation of side phases, such as cerium oxide (CeO_2) and calcium phosphate $Ca_3(PO_4)_2$ have been detected. It was demonstrated that infrared spectroscopy is very effective method to characterize the formation of CHAp. The SEM results showed that CHAp solids were homogeneous having small particle size distribution. The luminescent properties of these samples were also investigated. The position of the broad emission band at around 350 nm is almost independent on the Ce concentration, however, the intensity of photoluminescence peak slightly depends on the cerium concentration. In conclusion, Ce substituted CHAp samples show interesting luminescent properties and could be a good candidate for biocompatible drug carriers.

ACKNOWLEDGEMENTS

This research was funded by a grant (No. TAP LLT 07/2012) from the Research Council of Lithuania.

REFERENCES

1. S.V. Dorozhkin, J. Mater. Sci. **44**, 2343 (2009).
2. A. Bigi, E. Boanini, K. Rubini, *J. Solid State Chem*. **177**, 3092 (2004).
3. J. Liu, K. Li, H. Wang, M. Zhu, H. Yan, *Chem. Phys. Lett.* **396**, 429 (2004).
4. C.E. Fowler, M. Li, S. Mann, H.C. Margolis, *J. Mater. Chem*. **15**, 3317 (2005).
5. G. Goller, F.N. Oktar, S. Agathopoulos, D.U. Tulyaganov, J.M.F. Ferreira, E.S. Kayali, I. Peker, *J. Sol-Gel Sci. Technol*. **37**, 111 (2006).
6. I. Mayer, J.D.B. Featherstone, *J. Cryst. Growth* **219**, 98 (2000).
7. S. Ben Abdelkader, I. Khattech, C. Rey, M. Jemal, *Thermochim. Acta*. **376**, 25 (2001).
8. M. Wakamura, K. Kandori, T. Ishikawa, *Polyhedron* **16**, 2047 (1997).
9. *Idem., Colloids Surf.* **164**, 297 (2000).
10. A. Serret, M. V. Cabanas, M. Vallet-Regi, *Chem. Mater*. **12**, 3836 (2000).
11. F.B. Bagam Bisa, H.F . Kappert, W. Schili, *J. Oral. Maxillofac. Surg*. **52**, 52 (1994).
12. J. Livage, M. Henry, C. Sanchez, *Progr. Solid State Chem*. **18**, 259 (1988).
13. B.L. Cushing, V.L. Kolesnichenko, C.J. O'Connor, *Chem. Rev.* **104**, 3893 (2004).
14. J.D. Mackenzie, E.P. Bescher, *Acc. Chem. Res.* **40**, 810 (2007).
15. C. Yu, D. Cai, K. Yang, J.C. Yu, Y. Zhou, C. Fan, *J. Phys. Chem. Solids* **71**, 1337 (2010).
16. I. Bogdanoviciene, A. Beganskiene, K. Tõnsuaadu, J. Glaser, H-J. Meyer, A. Kareiva, *Mater. Res. Bull.* **41**, 1754 (2006).
17. I. Bogdanoviciene, K. Tõnsuaadu, A. Kareiva, *Polish J. Chem*. **83**, 47 (2009).
18. I. Bogdanoviciene, K. Tõnsuaadu, V. Mikli, I. Grigoraviciute-Puroniene, A. Beganskiene, A. Kareiva. *Centr. Eur. J. Chem.* **8**, 1323 (2010).
19. N. Pleshko, A. Boskey, R. Mendelsohn, *Biophys. J. Biophys. Soc.* **60**, 786 (1991).
20. J. Chen, Y. Wang, X. Chen, L. Ren, C. Lai, W. He, Q. Zhang, *Mater. Lett.* **65**, 1923 (2011).